Biosensors and Bioelectronics 126 (2019) 412–417

Contents lists available at ScienceDirect

Biosensors and Bioelectronics

journal homepage: www.elsevier.com/locate/bios

A facile electrochemical aptasensor for lysozyme detection based on target-induced turn-off of photosensitization

Zhaoxia Chen[a], Qiao Xu[a], Gangxu Tang[a], Shuang Liu[a], Shuxia Xu[b,c,*], Xinfeng Zhang[a,**]

[a] College of Materials and Chemistry & Chemical Engineering, Chengdu University of Technology, Chengdu 610059, China
[b] College of Environment and Ecology, Chengdu University of Technology, Chengdu 610059, China
[c] State Environmental Protection Key Laboratory of Synergetic Control and Joint Remediation for Soil & Water Pollution, Chengdu University of Technology, Chengdu 610059, China

ARTICLE INFO

Keywords:
Electrosensor
Photosensitization
Lysozyme
Aptamer

ABSTRACT

The quantification of proteins is essential in fundamental research or clinical applications. Here, we developed a facile electrochemical aptasensor based on target-induced turn-off of photosensitization for label-free and ultrasensitive detection of protein (exemplified by lysozyme). EB (ethidium bromide) molecules that were embedded in dsDNA between lysozyme binding aptamer and complementary DNA immobilized on the electrode, could photo-cleave the dsDNA via singlet oxygen (O_2^1) during photosensitization, resulting in a high voltammetry current of the $[Fe(CN)_6]^{3-/4-}$. Upon recognition of the lysozyme by aptamer, the EB molecules were released from dsDNA, and its photosensitization activity was turned off. As a result, more amount of complementary DNA was retained on the Au nanoparticles modified carbon nanotube paste electrode (AuNPs-CNPE), leading to a declined voltammetry current. Such a sensing strategy allowed detection of 10 pM-1 μM lysozyme with a low detection limit (about 2 pM). Besides, the sensor was free of labeling procedure as well as extra signal amplification step, and the CNPE modification was quite simple, only with AuNPs. The sensor also showed excellent selectivity toward lysozyme in the presence of interfering proteins, such as thrombin, bovine serum albumin, myoglobin, etc. The proposed sensor was applied to the determination of lysozyme in urine samples with the recoveries ranging from 96.6% to 101%. The proposed biosensor holds a great promise in developing other electrochemical sensors based on photosensitization.

1. Introduction

Lysozyme, an important protein, was widely distributed in diverse organisms, such as virus, bacteria, plants, insects, mammalian tissues and secretions. It is ubiquitous in cells, and its changes in level in serum or urine always indicate many diseases such as cancer (Sava et al., 1989), HIV (Lee-Huang et al., 2005) and inflammation (Ganz et al., 2003). Lysozyme can also potentially lead to allergic reactions in sensitive individuals even in trace amounts (Mainente et al., 2017). High performance liquid chromatography (HPLC) with UV/mass spectrometric detection mode is usually used for lysozyme quantification (Labella et al., 2016; Guarino et al., 2011; Fuselli et al., 2012), whereas the HPLC-based methods suffered from tedious sample preparation as well as long analysis time. Hence, development of facile biosensors has been given considerable significance for fast detection of protein including lysozyme.

Enzyme linked immunosorbent assay (ELISA) is one of the most frequently used for sensing of protein. However, it is limited by the availability of commercial antibodies. In place of commercial antibodies, the use of aptamers as the recognition elements may be an alternative strategy, as they are inexpensive, easily available and fast to use (Hamaguchi et al., 2001). Considerable efforts have been made to develop aptasensors using various detection methods such as colorimetry (Mishra et al., 2017; Song et al., 2011; Wang et al., 2010) fluorescence (F. Zhang et al., 2015; Liu et al., 2014; Wang et al., 2009), chemiluminescence (Li et al., 2011; Hun et al., 2010), surface plasmon resonance (Wang et al., 2011), etc. Electrochemical aptasensors offering short analytical time, high sensitivity and wide range of applications, have been demonstrated to be an appealing tool for lysozyme detection (Vasilescu et al., 2016). To facilitate detection of low abundant lysozyme, one of the effective approaches for signal amplification is modifying the electrode by functional nanomaterials like Au

* Corresponding author at: College of Environment and Ecology, Chengdu University of Technology, Chengdu 610059, China.
** Corresponding author.
E-mail addresses: xushux@cdut.edu.cn (S. Xu), zhangxinfeng09@cdut.cn (X. Zhang).

https://doi.org/10.1016/j.bios.2018.09.074
Received 7 July 2018; Received in revised form 9 September 2018; Accepted 20 September 2018
Available online 21 September 2018
0956-5663/

nanoparticles (Li et al., 2010), chitosan-graphene oxide (Erdem et al., 2014). TiO_2/three-dimensional reduced graphene oxide/polypyrrole nanocomposite (Wang et al., 2015). These modifications especially by multi-component nanomaterials, always required sophisticated procedures. DNA engineering techniques such as rolling circle amplification (Zhou et al., 2007), hybridization chain reactions (Chen et al., 2015), etc., are also good signal amplification strategies for protein detection, but always need careful design and extra amplification steps. Thus, new signal amplification procedure for electrochemical aptasensing of protein is still highly desirable.

In recent years, photosensitization, as a green catalytic amplification strategy, has played an important role in organic synthesis (Ischay et al., 2008), hydrogen preparation (Khnayzer et al., 2013) and pollutant degradation (Li et al., 2017). It also has been demonstrated to be a good catalytic signal amplification strategy for sensing (Xu et al., 2013; Zhang et al., 2014, 2018; Huang et al., 2018; Tang et al., 2017). Recently, we have developed a dsDNA-dye photosensitization technology and further used it for ultrasensitive visual or electrochemical sensing of DNA (X.F. Zhang et al., 2015; Qin et al., 2016). Additionally, label-free DNA detection can be readily achieved by formation of dsDNA during recognition of target DNA.

The aim of this work is to develop a target-induced photosensitization turn-off technique as a new catalytic signal amplification approach for label-free and ultrasensitive electrochemical detection of protein (exemplified by lysozyme). In the preliminary experiments, we found the EB molecules (Fig. S1) that were embed in dsDNA between aptamer and its complementary DNA (DNA-c) can effectively photocleave of DNA, leading to the fall of the DNA, and correspondingly, a high redox current of $[Fe(CN)_6]^{3-/4-}$ (Qin et al., 2016). Here, carbon nanotube paste electrode (CNPE) modified with gold nanoparticles (AuNPs) was fabricated and capture DNA (DNA-c) was immobilized on gold surfaces by means of self-assembly. Upon base paring between lysozyme binding aptamer (LBA) and DNA-c, dsDNA was formed and EB molecules were embedded into it. In the presence of lysozyme, the dsDNA-EB photosensitization system will be dissociated via the binding reaction between aptamer and lysozyme, and thus turning off the photosensitization. Accordingly, the DNA-c was retained in the electrode without cleavage, resulting in a low $[Fe(CN)_6]^{3-/4-}$ redox current (Fig. 1). Hence, label-free detection of lysozyme can be achieved by target-induced turn-off of photosensitization.

2. Experimental

2.1. Materials

All HPLC-purified oligonucleotides were purchased from Sangon Biotechnology Co. Ltd. (Shanghai, China) with the following sequences:

Complementary DNA (DNA-c): 5′-CTA AGT AAC TCT GCA CTC TTA TAT ATC ATA GAA TTG GTA GAT-$(CH_2)_6$-SH-3′.

Lysozyme binding aptamer (LBA): 5′-ATC TAC GAA TTC ATC AGG GCT AAA GAG TGC AGA GTT ACT TAG-3′.

Tris (hydroxymethyl) aminomethane (Tris), lysozyme (Lyz), thrombin, bovine serum albumin (BSA) were purchased from Sangon Biotechnology Co. Ltd. (Shanghai, China). Ethidium bromide (EB) was purchased from Alfa Aesar (USA). GO was supplied from Chengdu Organic Chemicals Co. Ltd. (Chengdu, China). Other chemicals used were of analytical grade and were supplied from Kelong reagent Co. (Chengdu, China). All solutions were prepared using 18.2 MΩ·cm ultrapure water.

2.2. Apparatus

Cyclic voltammetry (CV) and differential pulse voltammetry (DPV) measurements were performed with a CHI 660E electrochemical analyzer (Chenhua Instrument Shanghai Co., Ltd., China). The size and morphology of the electrode surface was characterized by a scanning electron microscope (SEM-EDX, XL30 and Philips, Netherland). Three-electrode system with carbon nanotube paste electrode (CNPE) as the working electrode, a Pt wire as auxiliary electrode and an Ag/AgCl electrode as reference electrode was applied for the experiments. A 3 W green LED (520–530 nm in emission wavelength) which was placed opposite of the working electrode, was used for initiating the photochemical reaction.

2.3. Preparation of unmodified carbon paste electrodes

Unmodified carbon paste was prepared by hand mixing of 80% of graphite powder and 20% of paraffin oil. The carbon nanotube paste (CNP) was prepared by mixing 80% (w/w) carbon nanotubes (CNTs) with 20% (w/w) paraffin in a mortar and pestle. The graphene-based carbon paste (G-CP) and graphene oxide-based carbon paste (GO-CP) consisted of 80% graphite powder or GO, and 20% paraffin oil by weight. Constituents were mixed thoroughly with a mortar and pestle until a thick paste was created. Unmodified carbon pastes were then forced into carbon paste electrodes (CPE) body with 3.0 mm internal diameter. Surfaces of the paste electrodes were smoothed by polishing on weighing papers whenever regeneration of the electrode was required. Fig. S2 showed that CNPE has optimum CV signal among the investigated different paste electrodes, CPE, G-CPE, GO-CPE and CNPE.

2.4. Fabrication of LBA/DNA-c/AuNPs/CNPE and electrochemical characterization

AuNPs with a diameter of 13 nm were prepared by the citrate reduction of $HAuCl_4$. Firstly, to construct the AuNPs modified CPE (AuNPs/CNPE), CNPE was modified by a drop of 30 μl of AuNPs solution. The scanning electron microscope (SEM) graphs of AuNPs/CNPE were shown in Fig. S3. Then the AuNPs/CNPE was placed into 1 μM complementary DNA (DNA-c) solution for 15 h at 4 °C. The electrode was then rinsed repeatedly with 10 mM Tris buffer to remove unbounded DNA strands, and the electrode of DNA-c/AuNPs/CNPE was obtained. After that, DNA-c/AuNPs/CNPE was incubated in 2 μM LBA for 2 h at room temperature, and the base pair interaction between DNA-c and LBA occurred with the formation of LBA/DNA-c/AuNPs/CNPE. The prepared LBA/DNA-c/AuNPs/CNPE was used for further lysozyme sensing.

All the processes of electrode modifying and aptamer immobilization were studied using CV and DPV techniques. CV was carried out at room temperature in 5 mM $[Fe(CN)_6]^{3-/4-}$ solution with 0.1 M KCl and 10 mM Tris as background electrolyte at a scan rate of 50 mV/s. DPV was performed at a potential scanned between 0.1 and 0.5 V with a modulation amplitude 25 mV and step potential 5 mV in 0.1 M KCl and 10 mM Tris.

2.5. Lysozyme sensing procedure

During the sensing, the prepared LBA/DNA-c/AuNPs/CNPE was immersed into a solution containing various concentration of lysozyme for 40 min at room temperature. Afterwards, the obtained LBA/DNA-c/AuNPs/CNPE was incubated in 1.2 mM EB solution for 20 min at room temperature. The EB/LBA/DNA-c/AuNPs/CNPE was rinsed repeatedly with Tris buffer and then immersed in the buffer, followed by 3 W green LED irradiation for 4 min. The resulted electrode was then transferred into the electrochemical system for CV and DPV measurements as the above.

3. Results and discussion

3.1. Fabrication of photocatalytic electrosensor for lysozyme detection

Fig. 1 illustrates the target-induced turn-off of photosensitization system for electrochemical detection of lysozyme. The DNA-c modified

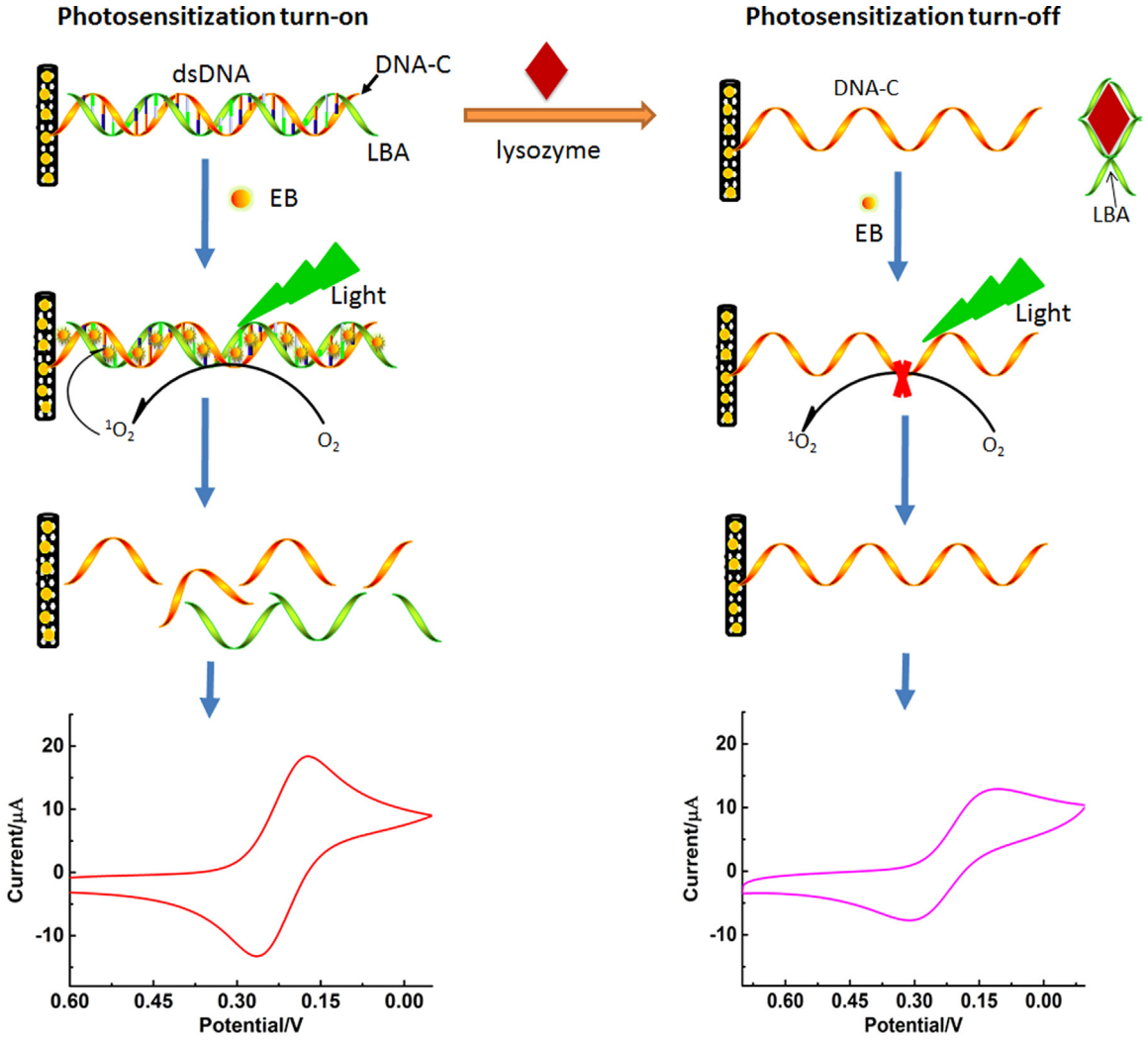

Fig. 1. Schematic illustration of target-induced turn-off of photosensitization.

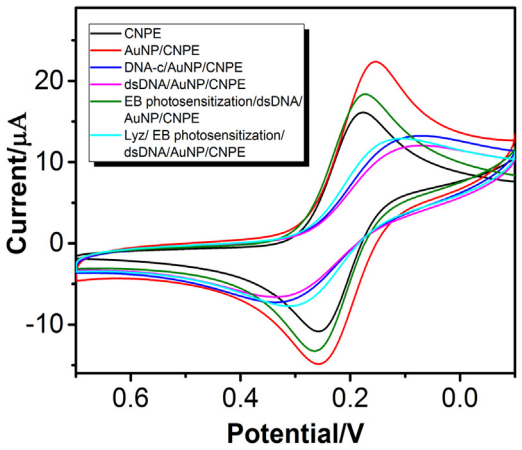

Fig. 2. CVs of $[Fe(CN)_6]^{3-/4-}$ at each modification/photocleaving steps. Experimental conditions: EB concentration, 1.0 mM; irradiation time, 7.5 min; incubation time of lysozyme, 30 min; and buffer solution, pH 7.4 of 10 mM Tris.

with thiol group was immobilized on the electrode through thiol-Au interaction. Further by base pairing, the double strand DNA (dsDNA between DNA-c and LBA) was assembled on the AuNPs. The dsDNA could trigger the photosensitization activity of EB under green LED irradiation and yielded singlet oxygen (O_2^1), as was proved in our previous study (Qin et al., 2016). The O_2^1 efficiently cleaved the dsDNA, so the less blocking of electrode and weaker charge repulsion effect led to a high peak current of $[Fe(CN)_6]^{3-/4-}$. In the presence of lysozyme, the specific binding of LBA to lysozyme denatured the duplex and liberated lysozyme-binding LBA into the solution. The lysozyme can cause the dissociation of the duplex, which was due to the fact that target-aptamer complex was more constant than the short DNA duplex (Li et al., 2010; Zou et al., 2007). EB molecules were released from dsDNA, and their photosensitization abilities were decreased, thus resulting in the turn-off of photosensitization. Because DNA-c cannot be cleaved in such case, the blocking effect to electrode and charge repulsion by DNA-c led to a deceased peak current of $[Fe(CN)_6]^{3-/4-}$. Accordingly, quantitative determination of lysozyme can be achieved by detecting the variation of $[Fe\ (CN)_6]^{3-/4-}$ peak current. In order to verify that the feasibility of the strategy, we tested the DPV of $[Fe\ (CN)_6]^{3-/4-}$ in the presence of 10 nM lysozyme, and Tris buffer solution was used as a control. The obviously decreased DPV current for 10 nM lysozyme demonstrated that the target-induced turn-off of photosensitization strategy is workable (Fig. S5).

3.2. The electrochemical characterization of the sensor surfaces

The CVs of $[Fe(CN)_6]^{3-/4-}$ at each modification/photocleaving steps were studied in 10 mM Tris (pH 7.4), as can be seen from Fig. 2. When dsDNA (DNA-c and LBA) was immobilized on the AuNPs/CNPE, both of

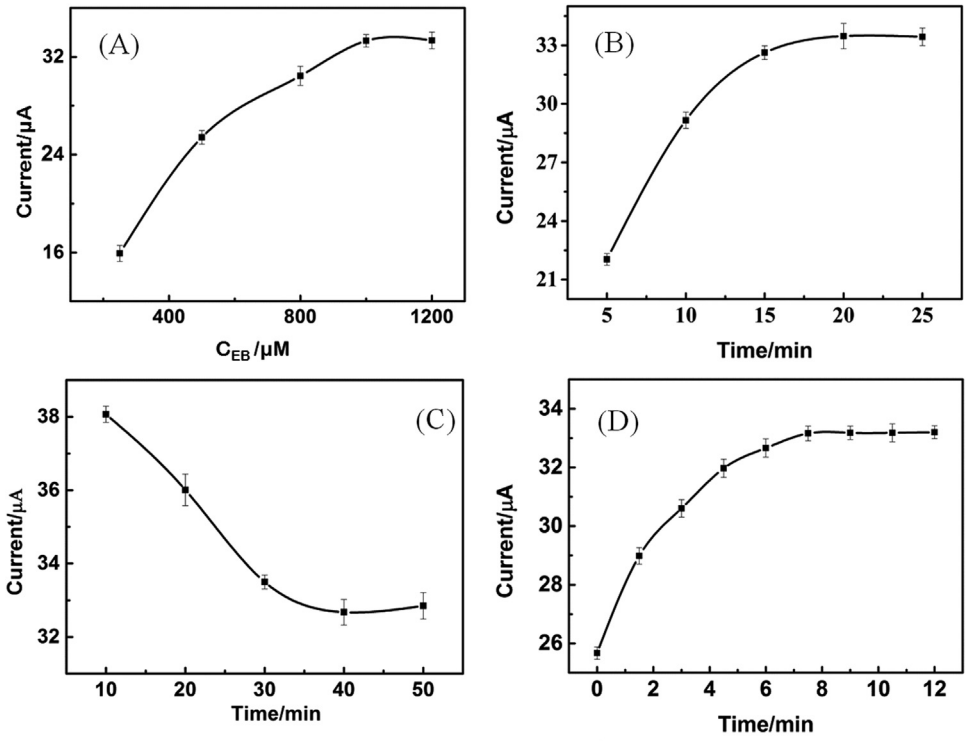

Fig. 3. Factors that influenced the photocatalytic activity (evaluated through the DPV current of $[Fe(CN)_6]^{3-/4-}$). EB concentration (A); incubation time of dsDNA with EB (B); incubation time of lysozyme (C); and LED irradiation time (D). Experimental conditions: DNA-c concentration, 2 μM; LBA concentration, 100 nM and buffer solution, pH 7.4 of 10 mM Tris. The error bar stands for the standard deviation of three parallel determinations.

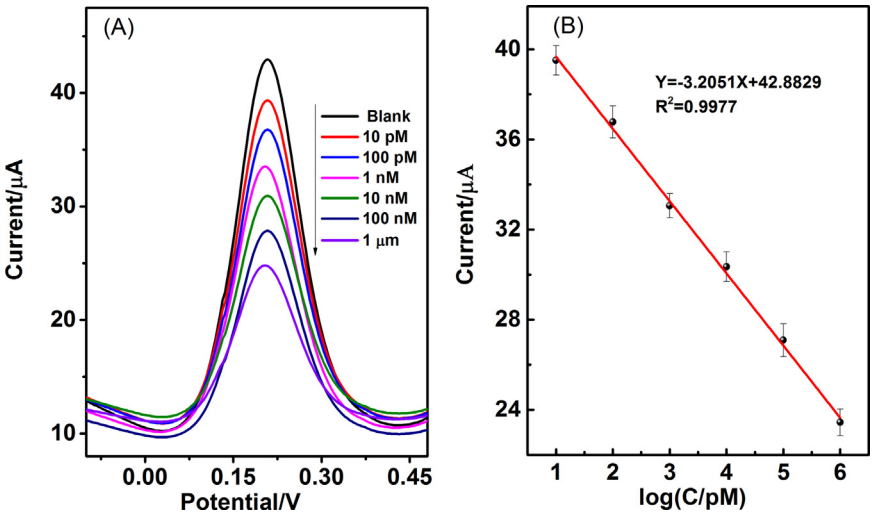

Fig. 4. Variation of the DPV under LED irritation with increasing concentration of lysozyme (A) and the linear relationship between peak currents and logarithmic lysozyme concentration (B). Experimental conditions: EB concentration, 1.0 mM; irradiation time, 7.5 min; incubation time of lysozyme, 30 min; and buffer solution, pH 7.4 of 10 mM Tris. The error bar stands for the standard deviation of three parallel determinations.

the anodic and cathodic peak currents of $[Fe(CN)_6]^{3-/4-}$ decreased. The reduction in peak current was due to that the negatively charged phosphate skeletons of the immobilized dsDNA on the electrode prevented $[Fe(CN)_6]^{3-/4-}$ from reaching the electrode surface by electrostatic repulsion. After photocleaving of the dsDNA by EB photosensitization, the peak currents of $[Fe(CN)_6]^{3-/4-}$ recovered. In the presence of lysozyme, it bound with LBA and led the dissociation of dsDNA , so turned off the photosensitization. Correspondingly, both of the anodic and cathodic peak currents remarkably decreased.

3.3. Optimization of photocatalytic sensing system

The experimental parameters that can affect the photocatalytic sensing system were optimized in terms of EB concentration, incubation time of EB, incubation time of lysozyme and LED irradiation time. The effect of EB concentration was investigated from 0.25 to 1.2 mM. As shown in Fig. 3 (A), the peak current increased as EB concentration increased in the range of 0.25–1.0 mM probably because more EB molecules that were embedded in the dsDNA. When EB concentration was higher than 1.0 mM, the peak current almost maintained constant. Thus, the optimal EB concentration was selected as 1.0 mM. The effect of EB incubation time was optimized from 5 to 25 min. Fig. 3 (B) showed that the peak current of $[Fe (CN)_6]^{3-/4-}$ increased from 5 to 20 min and then held constant as the incubation time was over 20 min, indicating that 20 min was suitable for the formation of EB-dsDNA complex. The effect of lysozyme incubation time was tested from 10 to 50 min. Fig. 3(C) indicated that the peak current of $[Fe(CN)_6]^{3-/4-}$ decreased from 10 to 30 min and then kept constant as the incubation time was over 30 min. The effect of irradiation time was also investigated in the range of 0–12 min (Fig. 3D). The peak current increased sharply as the irradiation time varied from 0 to 7.5 min, and longer irradiation time (> 7.5 min) only led to a slight enhancement of the peak current. Hence, 7.5 min was adequate in view of both high photocatalytic ability and fast analysis.

Table 1
Comparison of the proposed technique with other reported assays for the detection of lysozyme.

Electrode[a]	Detection	Comments	Linear range	LOD	Ref.
Chitosan-GO-GE	EIS	Electrode modified by chitosan-graphene oxide	0–3.7 μM	28.53 nM	(Erdem et al., 2014)
TiO_2/3D-rGO/PPy-GE	DPV	Electrode modified by TiO_2/3D-rGO/PPy	0.007–3.5 nM	5.5 pM	(Wang et al., 2015)
pcDNA-LBA-GE	EIS	Label-free and amplification-free	0.2–4.0 nM	70 pM	(Peng et al., 2009)
DNA duplex-GE	SWV	Immobilized DNA on electrode	7–30 nM	450 pM	(Chen and Guo, 2013)
Cu_2O/rGO/PpPG-GE	DPV	Electrode modified by Cu_2O/rGO/PpPG	0.01–200 nM	60 pM	(Fang et al., 2016)
AuNPs-DNA-GE	DPV	Labeled by AuNPs, amplified by AuNPs network	1 pM-10 nM	0.32 pM	(Cao et al., 2018)
Fc-DNA/LBA/AuNPs-GE		Tagged by Fc and amplified by AuNPs	0.1 pM-1 nM	0.1 pM	(Li et al., 2010)
DNA/AgNCs-GE	CV	Labeled by AgNCs, HCR amplification	0.1 pM-10 nM	42 pM	(Chen et al., 2015)
TiO_2/PPAA-GE	EIS	Plasma modification, Electrode modified TiO_2/PPAA	3.5 pM-7 nM	1.04 pM	(Z. Zhang et al., 2015)
dsDNA-EB-CNPE	DPV	Photosensitization, Electrode modified by only AuNPs	10 pM- 1μM	2 pM	This work

[a] Abbreviations: GE = gold electrode; rGO = reduced grapheme oxide; PPy = polypyrrole; pcDNA = partial complementary single strand DNA; PpPG = plasma-polymerized propargylamine; PPAA = polyacrylic acid; HCR = hybridization chain reaction.

3.4. Analytical performance of the lysozyme electrosensor

3.4.1. Linearity and limit of detection

Fig. 4 demonstrates the effect of different lysozyme concentrations on the biosensor response. With an increase of the lysozyme concentration, the peak current rose correspondingly. The linear response was obtained when the lysozyme concentrations were within the range of 10 pM-1 μM. The regression equation is the regression equation is $Y = 3.4019X + 5.4859$, with a correlation coefficient $R > 0.990$. Where Y is the reduction current of $[Fe(CN)_6]^{3-/4-}$; X is the logarithm of lysozyme concentration. The limit of detection (LOD, 3σ) of the developed biosensor for lysozyme was calculated to be about 2 pM. The comparison between the photocatalytic sensor and the reported electrochemical sensors for lysozyme detection was summarized in Table 1. Although our sensor is not as sensitive as some of the reported electrochemical assays, it was free of labeling procedure as well as extra signal amplification procedure such as hybridization chain reaction (HCR) or AuNPs networks; also the CNPE modification is quite simple, only by AuNPs.

The reproducibility of the sensor for lysozyme determination was investigated with intra-/inter-assay precision. The intra-assay precision, or the repeatability of the sensor, was evaluated by assaying 10 nM lysozyme with the same AuNPs/CNPE. The relative standard deviation (RSD) for 5 successive determinations was about 3.6%, demonstrating an excellent detecting repeatability. Moreover, the inter-assay precision, or the reproducibility, was estimated by detecting 10 nM lysozyme with five biosensors prepared in the same method independently, and the RSD was 4.7%. Thus, the proposed method had an excellent reproducibility for lysozyme determination. The good reproducibility maybe attributed to simple electrode modification and free of signal amplification procedure.

3.4.2. Stability

The storage stability of the designed sensor was also explored. For detection of 10 nM lysozyme, there was no significant current change (3.4%) in the first 7 h. The current response varied about 10.6% after 7-day period comparing to that of the initially fabricated electrode. These results indicated that the proposed biosensor had an acceptable stability.

3.4.3. Specificity

The specificity test was carried out by measuring and comparing the response of lysozyme with specific interferential biomolecules. When 10 nM each of lysozyme, 100 nM thrombin, BSA, myoglobin, ATP and glucose were incubated and detected individually with the electrosensor. As we can see from Fig. 5, only lysozyme can lead to the turn-off of the photosensitization, and resulted in a much lower current compared with those of the other interferential biomolecules. These results indicated that our biosensor was able to recognize lysozyme as the target with high specificity and can be used for selective detection of lysozyme.

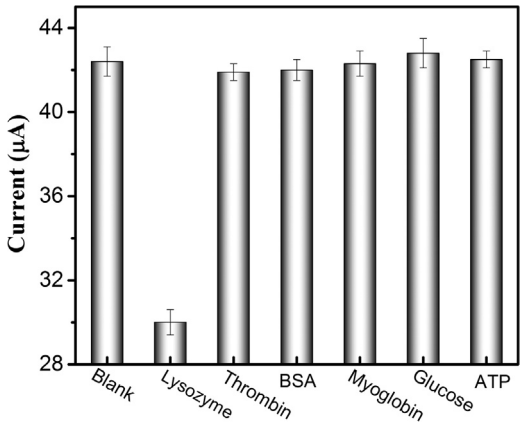

Fig. 5. Selectivity of the system for lysozyme analysis. Experimental conditions: EB concentration, 1.0 mM; irradiation time, 7.5 min; incubation time of lysozyme, 30 min; and buffer solution, pH 7.4 of 10 mM Tris. The error bar stands for the standard deviation of three parallel determinations.

3.4.4. Analysis of spiked urine sample

To examine the feasibility of the proposed sensor for possible application in real samples, the 10-fold diluted human urine samples from healthy individuals were tested. Four urine samples spiked with 0.1, 1, 20 and 100 nM lysozyme were detected by DPV. Recoveries were shown in Table S1, ranging from 96.6% to 101.1%. In the test, each sample underwent six parallel measurements, and the RSD was below 5%, suggesting a good reproducibility. These results indicated the applicability of the proposed method for lysozyme detection in real samples.

4. Conclusion

We have developed a target-induced turn-off of photosensitization technique *via* release of EB molecules from dsDNA during the lysozyme recognition by aptamer. Using electrochemical detection, the strategy allowed label-free and amplified sensing of lysozyme with a low LOD about 2 pM. The sensor is free of extra signal amplification procedure and the electrode modification is also quite simple, only by AuNPs. Although the LBA/DNA-c/AuNPs/CNPE cannot be reusable, the disposability of the CNPE also makes the sensing procedure be convenient. By altering the aptamer sequence, the electrochemical aptasensor will be also a promising tool for detection of other proteins or small biomolecules.

Acknowledgements

The authors gratefully acknowledge the financial support from the National Natural Science Foundation of China (Nos. 21475013 and 21305009), and the Sichuan Science and Technology Project (No. 2018JY0466).

Appendix A. Supporting information

Supplementary data associated with this article can be found in the online version at doi:10.1016/j.bios.2018.09.074.

References

Cao, X., Xu, J., Xia, J., Zhang, F., Wang, Z., 2018. Sens. Actuators B 255, 2136–2142.
Chen, L., Sha, L., Qiu, Y., Wang, G., Jiang, H., Zhang, X., 2015. Nanoscale 7 (7), 3300–3308.
Chen, Z., Guo, J., 2013. Electrochim. Acta 111, 916–920.
Erdem, A., Eksin, E., Muti, M., 2014. Colloid Surf. B 115, 205–211.
Fang, S., Dong, X., Ji, H., Liu, S., Yan, F., Peng, D., He, L., Wang, M., Zhang, Z., 2016. Microchim. Acta 183 (2), 633–642.
Fuselli, F., Guarino, C., La Matia, A., Longo, L., Faberi, A., Marianella, R.M., 2012. J. Chromatrogr. B 906, 9–18.
Ganz, T., Gabayan, V., Liao, H.I., Liu, L., Oren, A., Graf, T., Cole, A.M., 2003. Blood 101 (6), 2388–2392.
Guarino, C., Fuslli, F., La Mantia, A., Longo, L., 2011. Food Chem. 127 (3), 1294–1299.
Hamaguchi, N., Ellington, A., Stanton, M., 2001. Anal. Biochem. 294 (2), 126–131.
Huang, C., Fan, X., Yuan, Q., Zhang, X., Hou, X., Wu, P., 2018. Talanta 185, 258–263.
Hun, X., Chen, H., Wang, W., 2010. Biosens. Bioelectron. 26 (1), 248–254.
Ischay, M.A., Anzovino, M.E., Du, J., Yoon, T.P., 2008. J. Am. Chem. Soc. 130 (39), 12886–12887.
Khnayzer, R.S., McCusker, C.E., Olaiya, B.S., Castellano, F.N., 2013. J. Am. Chem. Soc. 135 (38), 14068–14070.
Lee-Huang, S., Maiorov, V., Huang, P.L., Ng, A., Lee, H.C., Chang, Y.T., Kallenbach, N., Chen, H.C., 2005. Biochemistry 44 (12), 4648–4655.
Labella, C., Lelario, F., Bufo, S.A., Musto, M., Frechi, P., Cosentino, Carlo, 2016. J. Food Nutr. Res. 55 (3), 263–269.
Li, L.D., Chen, Z.B., Zhao, H.T., Guo, L., Mu, X., 2010. Sens. Actuators B 149 (1), 110–115.
Li, Y., Pan, Y., Lian, L., Yan, S., Song, W., Yang, X., 2017. Water Res. 109, 266–273.
Li, Y., Qi, H., Gao, Q., Zhang, C., 2011. Biosens. Bioelectron. 26 (5), 2733–2736.
Liu, S., Na, W., Pang, S., Shi, F., Su, X., 2014. Analyst 139 (12), 3048–3054.
Mainente, F., Simonato, B., Pasini, G., Franchin, C., Arrigoni, G., Rizzi, C., 2017. Food Addit. Contam. A 34 (2), 145–151.
Mishra, R.K., Hayat, A., Mishra, Catanante, G.K., Sharma, G.V., Marty, J.L., 2017. Talanta 165, 436–441.
Peng, Y., Zhang, D., Li, Y., Qi, H., Gao, Q., Zhang, C., 2009. Biosens. Bioelectron. 25 (1), 94–99.
Qin, X.J., Xu, S.X., Deng, L., Huang, R.F., Zhang, X.F., 2016. Biosens. Bioelectron. 85, 957–963.
Sava, G., Benetti, A., Ceschia, V., Pacor, S., 1989. Anticancer Res. 9 (3), 583–591.
Song, Y., Xu, C., Wei, W., Ren, J., Qu, X., 2011. Chem. Commun. 47 (32), 9083–9085.
Tang, S., Wang, M., Li, Z., Tong, P., Chen, Q., Li, G., Chen, J., Zhang, L., 2017. Biosens. Bioelectron. 89 (2), 866–870.
Vasilescu, A., Wang, Q., Li, M., Boukherroub, R., Szunerits, S., 2016. Chemosensors 4 (2), 10.
Wang, L., Li, L., Xu, Y., Cheng, G., He, P., Fang, Y., 2009. Talanta 79 (3), 557–561.
Wang, M., Zhai, S., Ye, Z., He, L., Peng, D., Feng, X., Yang, Y., Fang, S., Zhang, Zhang, H.Z., 2015. Dalton Trans. 44 (14), 6473–6479.
Wang, X., Xu, Y., Chen, Y., Li, L., Liu, F., Li, N., 2011. Anal. Bioanal. Chem. 400 (7), 2085–2091.
Wang, Y., Pu, K.Y., Liu, B., 2010. Langmuir 26 (12), 10025–10030.
Xu, S.X., Zhang, X.F., Liu, W.W., Sun, Y.H., Zhang, H., 2013. Biosens. Bioelectron. 43, 160–164.
Zhang, F., Zhao, Y.Y., Chen, H., Wang, X.H., Chen, Q., He, P.G., 2015a. Chem. Commun. 51 (30), 6613–6616.
Zhang, X.F., Deng, L., Huang, C.P., Zhang, J., Hou, X.D., Wu, P., Liu, J., 2018. Chem.-Eur. J. 24 (11), 2602–2608.
Zhang, X.F., Huang, C.P., Xu, S.X., Chen, J., Zeng, Y., Wu, P., Hou, X.D., 2015b. Chem. Commun. 51 (77), 14465–14468.
Zhang, X.F., Zhang, H., Xu, S.X., Sun, Y.H., 2014. Analyst 139 (1), 133–137.
Zhang, Z., Zhang, S., He, L., Peng, D., Yan, F., Wang, M., Zhao, J., Zhang, H., Fang, S., 2015c. Biosens. Bioelectron. 74, 384–390.
Zhou, L., Ou, L.J., Chu, X., Shen, G.L., Yu, R.Q., 2007. Anal. Chem. 79 (19), 7492–7500.
Zou, X., Song, S., Zhang, S., Pan, D., Wang, L., Fan, C., 2007. J. Am. Chem. Soc. 129, 1042–1043.